Ti-2007 Science and Technology, edited by M. Ninomi, S. Akiyama, M. Ikeda, M. Hagiwara, K. Maruyama
The Japan Institute of Metals (2007)

Dynamic Recrystallization in Titanium Alloys during Hot Deformation

Tadashi Furuhara[1], Hiroshi Abe[2], Behrang Poorganji[3], Tadashi Maki[4]

[1]*Institute for Materials Research, Tohoku University, 2-1-1 Katahira, Aoba-ku, Sendai 980-8577, Japan*
[2]*Formerly Graduate Student, Kyoto University, now at Toyota Motor Corporation, Japan*
[3]*Graduate Student, Tohoku University, 2-1-1 Katahira, Aoba-ku, Sendai 980-8577, Japan*
[4]*Emeritus Professor, Kyoto University, now at Nippon Steel Corporation, Futtsu 293-8511, Japan*

Microstructure change of β titanium alloys, Ti-15V-3Cr-3Sn-3Al and Ti-10V-2Fe-3Al and an (α+β) titanium alloy, Ti-6Al-4V, during hot deformation at temperatures in β single-phase and (α+β) two-phase regions was studied. For the β titanium alloys, dynamic recovery takes place dominantly within β grains during deformation in the β single-phase region although some discontinuous dynamic recrystallization occurs along β grain boundaries. The size and fraction of recrystallized β grains increase as the strain rate decreases or the deformation temperature becomes higher. When deformation was applied just below the β transus, a small fraction of α phase precipitates at β grain boundaries and suppresses discontinuous dynamic recrystallization. On the contrary, when the specimen is deformed at a lower temperature with a larger α volume fraction, continuous dynamic recrystallization occurs uniformly in the β matrix and most of the β subgrain boundaries formed in the early stage of deformation by dynamic recovery turn to high-angle ones by further deformation. As a result, (α+β) microduplex structures with α grain sizes of about 1μm are obtained. When lamellar (α+β) structures of Ti-6A1-4V are deformed in the (a+β) two phase regions where α phase is the majority, continuous dynamic recrystallization occurs in α resulting in gradual α globularization. A higher deforming temperature, a slower strain rate or refinement of initial α plate results in more extensive α globularization.

Keywords: titanium alloy, dual phase material, hot deformation, deformation, recovery, recrystallization, grain boundary

1. Introduction

Hot deformation of titanium alloys by rolling or forging is conventionally performed in β single-phase and (α+β) two-phase regions [1] mainly for β grain refinement beneficial for improvement of strength-ductility balance [2]. During such deformation, dynamic recovery (DRC) and dynamic recrystallization (DRX) take place. It is known that DRX is quite effective in the grain refinement when deformation is performed at a higher strain rate and a lower temperature, i.e. a lower Z (Zener-Hollomon parameter; $Z = \dot{\varepsilon} \exp(Q/RT)$) condition. However, DRX occurs in a narrow processing window inside the β single-phase region in the studies of flow stress in titanium and its alloys [1, 3-7]. In β titanium alloys, the occurrence of dynamic or meta-dynamic recrystallization was proposed for multi-pass forging [8]. Formation of recrystallized grains at β grain boundaries is characterized as a discontinuous DRX. It was also considered that DRX does not occur in (α+β) processing [9, 10].

Much attention has been paid to DRX as one of dominant mechanisms in the formation of ultra-fine grains by severe plastic deformation in ferrous alloys [11-14]. Continuous DRX, which accompanies nucleation of recrystallized grains of a high density and is completed without much grain growth, is proposed as the DRX mode operative in those studies. The present authors examined hot deformed microstructures of β titanium alloys in the β single-phase and (α+β) two-phase regions by means of scanning electron microscopy (SEM) and transmission electron microscopy (TEM) [15, 16]. Local orientation measurement revealed that β subgrain boundaries (low-angle boundaries) formed in the early stage of deformation by DRC becomes high-angle boundaries by further deformation in the (α+β) two phase region. However, the microstructures formed by dynamic restoration during hot deformation are still not well characterized in titanium alloys and necessary to be re-examined in accordance with the recent consideration on DRX mechanisms.

The present study summarizes the dynamic restoration mechanisms of representative titanium alloys during hot deformation at various temperatures and strain rates based upon local orientation measurements.

2. Experimental Procedure

Chemical compositions of the alloys used are listed in Table 1. The β transus temperatures are approximately 1023K for Ti-15V-3Cr-3Sn-3Al, 1053K for Ti-10V-2Fe-3Al and 1273K for Ti-6Al-4V, respectively. β solution treatments were performed at 1173K for 3.6ks after 60% cold rolling for Ti-15V-3Cr-3Sn-3Al and at 1123K for 3.6ks for Ti-10V-2Fe-3Al. By those solution treatments, equi-axed β structures were obtained, of which average grain sizes are 126μm for Ti-15V-3Cr-3Sn-3Al and 141μm for Ti-10V-2Fe-3Al, respectively. For Ti-6Al-4V, a β solution treatment was performed at 1323K for 1.8ks, resulting in a β grain size of 384pm, followed by furnace cooling (F.C.) or air cooling (A.C.) to obtain lamellar (α+β) structures and by water quenching (W.Q.) to obtain a martensite structure. After the β solution treatments, the specimens were isothermally held for 1.8ks at various temperatures in the β single-phase region or the (α+β) two-phase region and subsequently compressed at the same

Table 1. Chemical compositions of the materials used (mass%)

Alloy	V	Cr	Sn	Al	Fe	O	N	H	Ti
Ti-10V-2Fe-3Al	9.67	-	-	3.04	1.81	0.063	0.0086	0.0010	bal.
Ti-15V-3Cr-3Sn-3Al	15.2	2.99	2.97	3.04	0.203	0.114	0.0092	0.0187	bal.
Ti-6Al-4V	4.1	-	-	6.2	0.30	0.20	0.0055	0.0044	bal.

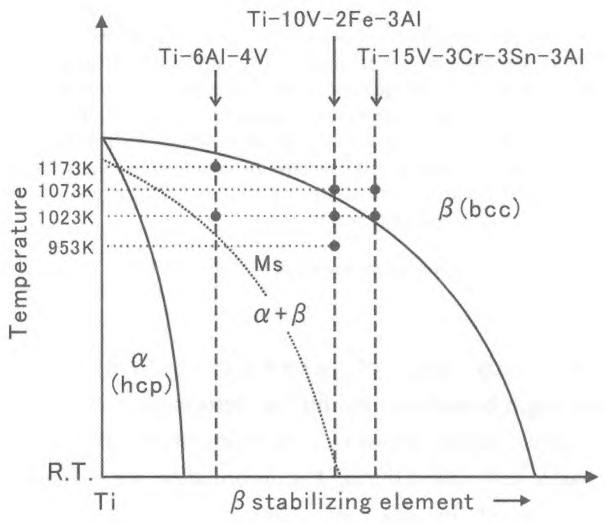

Figure 1. Deformation temperatures chosen in the present study.

temperature at initial strain rates between $4.2x10^{-1}$ ~ $4.2x10^{-5}$ s^{-1} up to 55% or 75% reduction. Fig. 1 summarizes the deformation temperatures chosen. After the hot compression, the specimens were immediately quenched by water.

Microstructures were observed with an optical microscope, SEM (Hitachi S3100H, Jeol JSM-6500F) and TEM (Philip CM200). Grain orientations were analyzed by means of electron backscatters diffraction (EBSD) in SEM and convergent beam Kikuchi diffraction (CBKD) in TEM.

3. Results and Discussion

3.1. Deformation of β Titanium Alloys [15, 16]

Figure 2(a) is an optical micrograph of the β solution-treated Ti-15V-3Cr-3Sn-3Al showing an equi-axed β structure obtained. The Ti-10V-2Fe-3Al specimens consisted of a similar β structure prior to hot compression at 1073K. At 1023K (Fig. 2(b)), a small amount of α phase precipitates along the β grain boundaries. At 953K (Fig. 2(c)), in addition to grain boundary α precipitation, fine, lath-shaped intragranular α precipitates are formed within β grains. However, the volume fraction of α phase in the initial microstructure before deformation is less than the

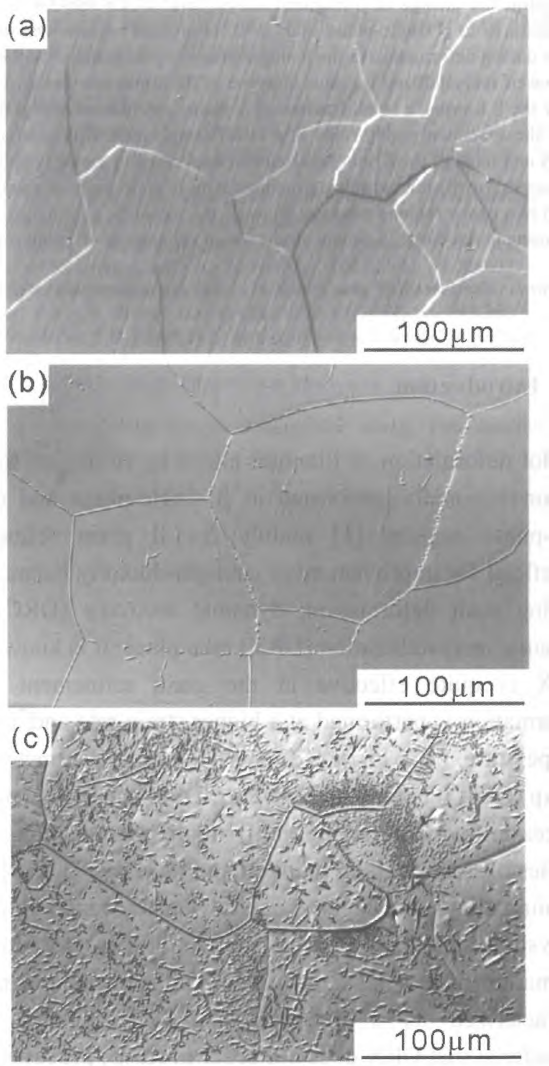

Figure 2. Optical microstructures just prior to hot compression; (a) Ti-15V- 3Cr-3Sn-3Al after the β solution treatment at 1173K for 3.6ks, (b) Ti-10V- 2Fe-3Al after holding at 1023K and (c) at 953K for 1.8ks, respectively.

equilibrium one at each temperature in the (α+-β) two-phase region, i.e., 10% at 1023K and 30% at 953K.

Figure 3(a) shows the optical microstructure of the Ti-15V-3Cr-3Sn-3Al specimen deformed by 55% compression at 1073K and an initial strain rate of $4.2x10^{-3}$ s^{-1}. Original β grains are elongated perpendicular to the compression axis (C.A.) and β grain boundaries become

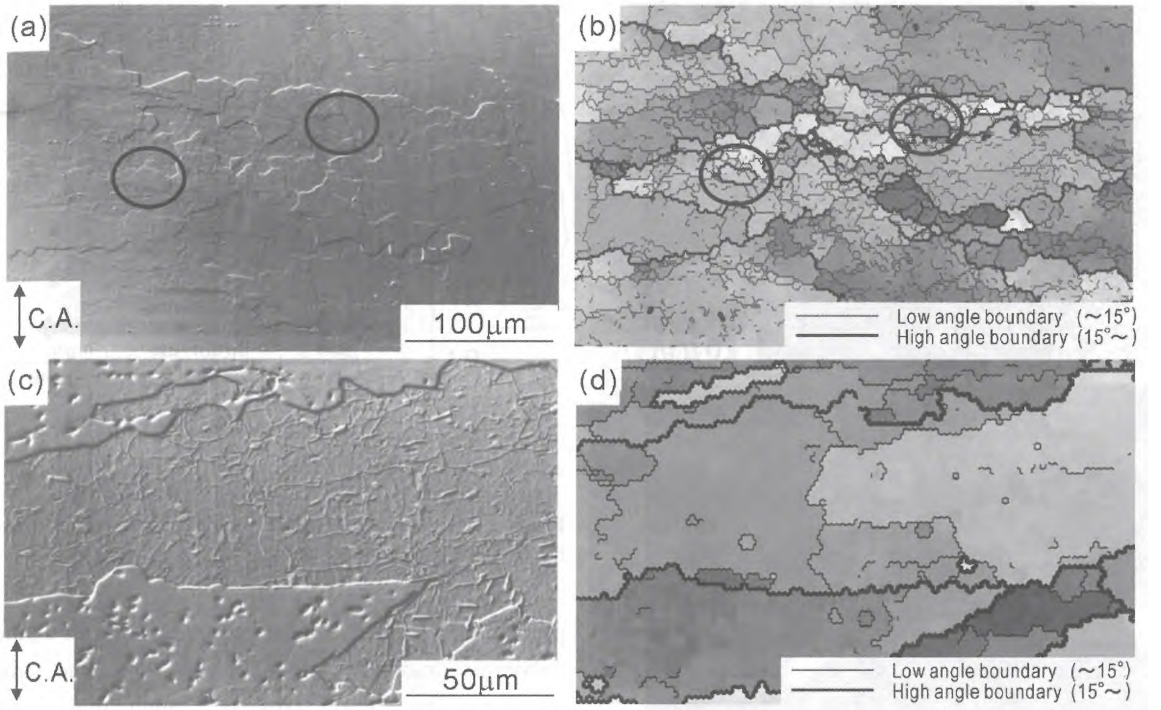

Figure 3. (a) Optical microstructure of Ti-15V-3Cr-3Sn-3Al deformed at 1073K by 55% compression at an initial strain rate of 4.2 $x10^{-3}$ s^{-1} and (b) the corresponding orientation map of β phase, (c) optical microstructure and (d) the corresponding orientation map of Ti-10V-2Fe-3Al deformed at 1023K by 55% compression at an initial strain rate of 4.2 $x10^{-5}$ s^{-1} (C.A.: Compression Axis).

wavy by strain-induced grain boundary migration. Those β grains containing many low-angle boundaries (see the orientation map of Fig. 3(b)) indicates that DRC mainly takes place at this deformation condition. Some equi-axed β grains are newly formed along original β grain boundaries as encircled in Figs. 3(a) and (b). In the map of Fig. 3(b), those β grains are clearly bounded by high-angle boundaries, and also contain subgrains within them. This clearly implies that those β grains are formed by DRX. The characteristic of this microstructure is typical of discontinuous DRX. A fraction or a size of the recrystallized β grain increases as a deformation temperature increases or a strain rate decreases. Similar deformed structures were observed in the case of Ti-10V-2Fe-3Al deformed in the β single phase region. Figures 3(c) and (d) are an optical micrograph and the corresponding orientation map of Ti-10V-2Fe-3Al deformed by 55% compression at 1023K and 4.2$x10^{-5}$ s^{-1}. This temperature is just below the β transus. Although some wavy grain boundaries are seen, elongated original β grains exhibit a fully recovered structure and equi-axed grains are hardly observed. This indicates that DRC only takes place in this specimen. It is considered that the migration of original β grain boundaries is suppressed by grain boundary α Precipitation and thus, discontinuous DRX does not occur this deformation temperature.

Figure 4 shows the microstructures of Ti-10V-2Fe-3A1 deformed by 55% compression at 953K and 4.2$x10^{-4}$ s^{-1}. In the optical micrograph of Fig. 4(a), original β grains appear to be still elongated but fine and uniform dispersion of α precipitates is obtained, as reported previously [17]. In TEM (Fig. 4(b)), β matrix consists of fine grains with grain size of about 1μm. The CBKD-TEM analysis has revealed that the boundaries between those β grains are mostly high- angle ones. Figure 4(c) shows the change in β grain boundary misorientation during deformation at 953K. In the early stage, low-angle β. boundaries are formed by DRC. However, the boundary misorientation increases gradually during deformation, leading to formation of the (α+β) microduplex structure consisting of high-angle β boundaries after the compression by 55% (ε = 0.7). This microstructure change at 953K is typical of continuous DRX. The presence of α phase which is harder than β phase [18] should enhance the DRX of β with small amounts of deformation. In Ti-10V- 2Fe-3Al, the equilibrium volume fraction of α phase is higher at 953K (ca. 30%) than at 1023K (ca. 10%). Therefore, continuous DRX in the β matrix should occur at 953K more easily.

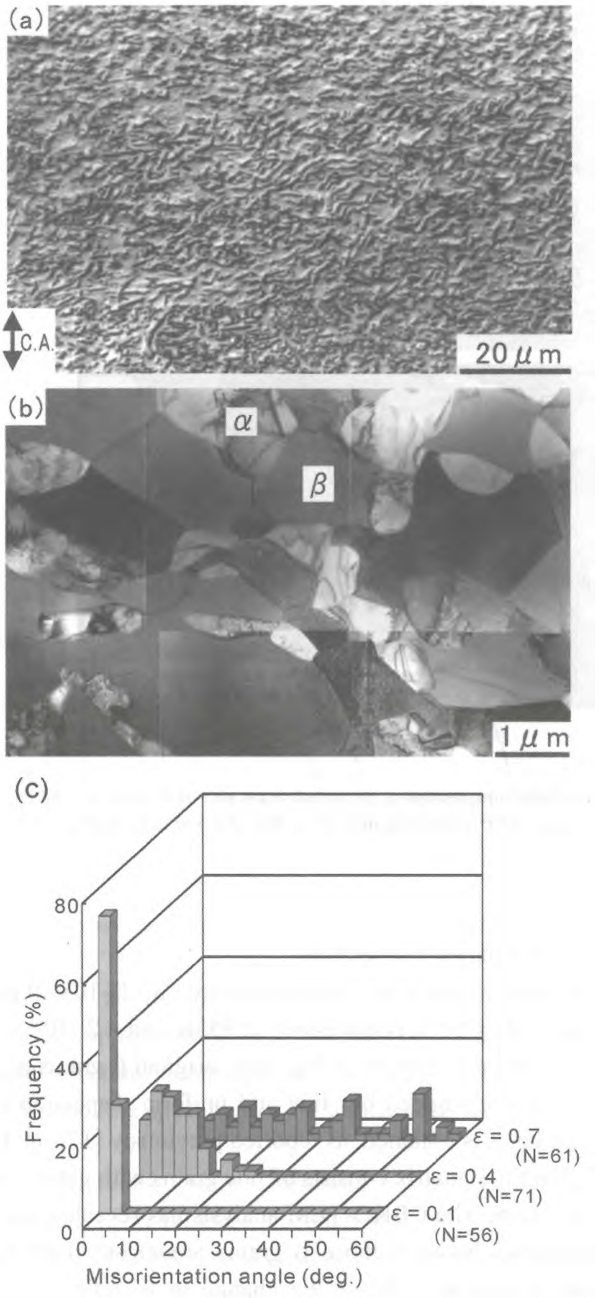

Figure 4. (a) Optical and (b) TEM microstructure of Ti-10V-2Fe-3Al deformed at 953K by 55% compression (initial strain rate: 4.2×10^4 (C.A.: Compression Axis), (c) change in misorientation across the β boundary during deformation.

Figure 5 shows the relationship between the sizes of DRX βgrains and β subgrains in Ti-15V-3Cr-3Sn-3A1 and Zener-Hollomon parameter ($Z = \dot{\varepsilon} \exp(Q/RT)$). There is a good correlation between them even in the early stage of DRX, indicating that high Z deformation is useful to refine the β grain size. However, the fraction of recrystallized β grain was smaller for a higher Z condition. It is presumably because the critical strain necessary for completion of DRX increases with the Z value [19]. In Fig. 5, the sizes of DRX β grains in Ti-10V-2Fe-3Al deformed at 953K are also

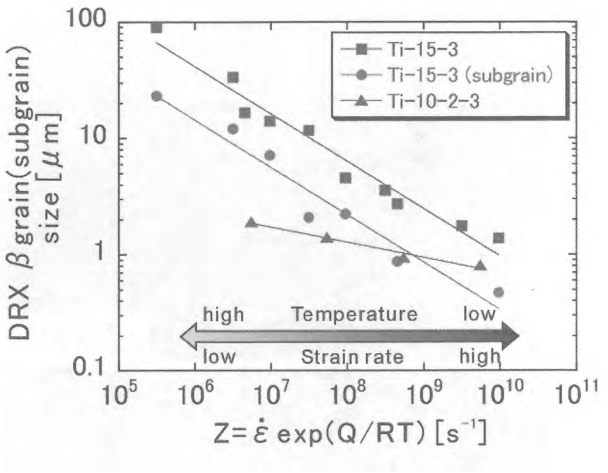

Figure 5. Relationship between Z parameter and sizes of dynamically recrystallized β grain and β subgrain.

plotted. The β grain sizes are around 1-2μm in diameter and decreases gradually as the Z value (i.e. the strain rate) increases. Those grain sizes were much smaller than those of the discontinuously recrystallized ones of Ti-15V-3Cr-3Sn-3Al at a given Z value in most of the range examined, and more close to the β subgrain sizes. α precipitates promote the transition of β grain boundary structure from the low-angle to high-angle one through the continuous DRX and furthermore, suppress the migration of β (sub) grain boundaries. Thus, it is reasonable that the DRX β grain size in Ti-10V-2Fe-3Al is similar to or finer than that of the subgrain size in Ti-15V-3Cr-3Sn-3Al deformed in the β single phase region.

3.2. Deformation of Ti-6A1-4V alloy

The microstructures of β solution treated and cooled specimens were Widmanstätten α plate structures in the F.C. and A.C. specimens whereas martensite structure was obtained in the W.Q. one. In each case, β matrix was partially retained. The structures after the isothermal holding at deformation temperatures were (α+β) lamellar structures formed by the growth of β matrix between α plates (Fig. 6). The volume fraction of α phase is approximately 80% at 1023K and 40~50% at 1173K. As a cooling rate increases, an interlamellar spacing of the lamellar structure and a thickness of α become finer.

It was found that hot deformed microstructures are quite heterogeneous [20], as seen typically in an optical micrograph of Fig. 7, regardless of the deformation conditions employed. The specimens compressed by 55% consist of three different structures, (1) fine elongated a lamella (EL) perpendicular to the compression axis, (2) irregularly bent α lamella (IBL) and (3) equi-axed α grains (EG), each of which is highlighted on the micrograph.

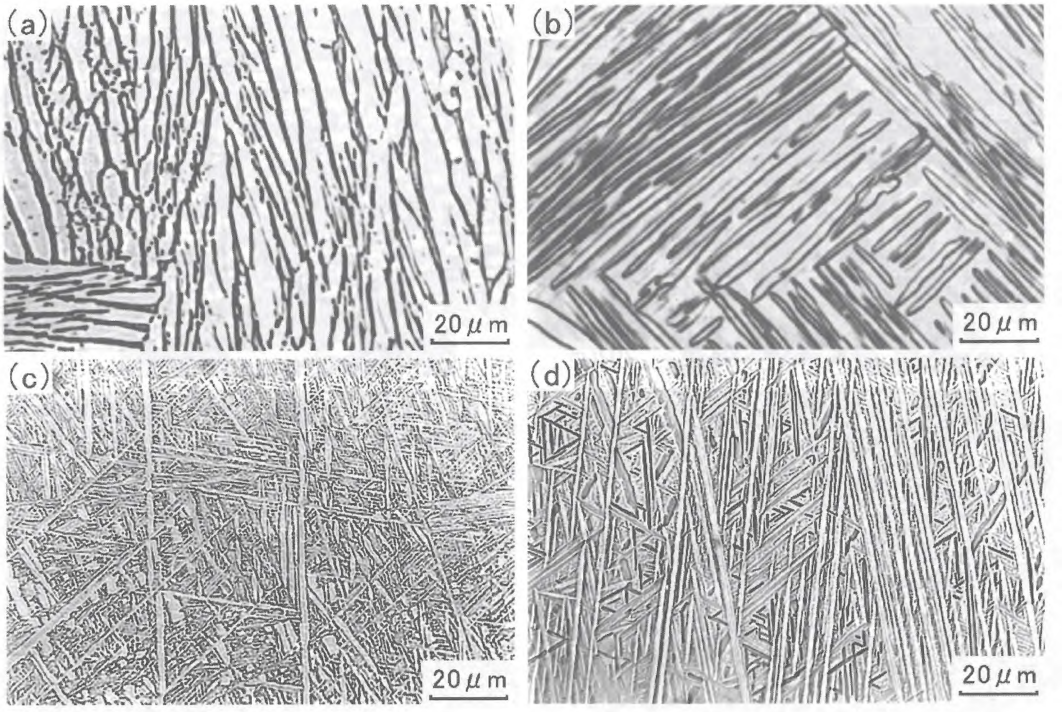

Figure 6. Optical micrographs of Ti-6Al-4V before compression; (a), (b) F.C. specimens annealed for 1.8ks at 1023K and 1173K, respectively; (c), (d) W.Q. specimens annealed for 1.8ks at 1023K and 1173K, respectively.

Fig. 8 shows the microstructure change of the WQ specimen during deformation at 1173K and 1123K, respectively. When the specimen is compressed by 55% (Fig. 8(a)), many low-angle α boundaries are seen in the α plates indicates that DRC mainly occurs in the α phase. Some high-angle boundaries were observed in the region where the α plates are largely bent. As deformation proceeds, the boundary misorientation in α phase increases gradually, resulting in formation of high-angle α boundaries and globularization of α phase. After 75% compression, most of the α boundaries become high-angle ones and α globularization is nearly completed as seen in Fig. 8(b). The size of the equi-axed α grain, ca. l-2μm, is nearly the same as the initial α plate thickness. For a higher deforming temperature, a slower strain rate and a finer initial structure prior to deformation, the degree of α globularization is

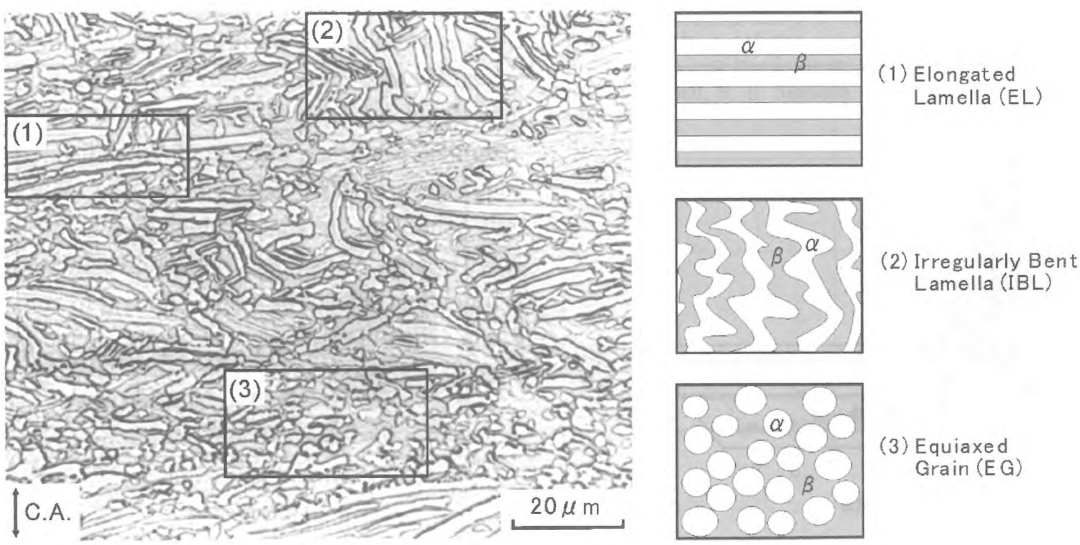

Figure 7. Optical microstructure and schematic illustration of the typical deformed structures in Ti-6Al-4V water-quenched and compressed at 1173K and $4.2x10^{-3}$ s^{-1} by 55%.

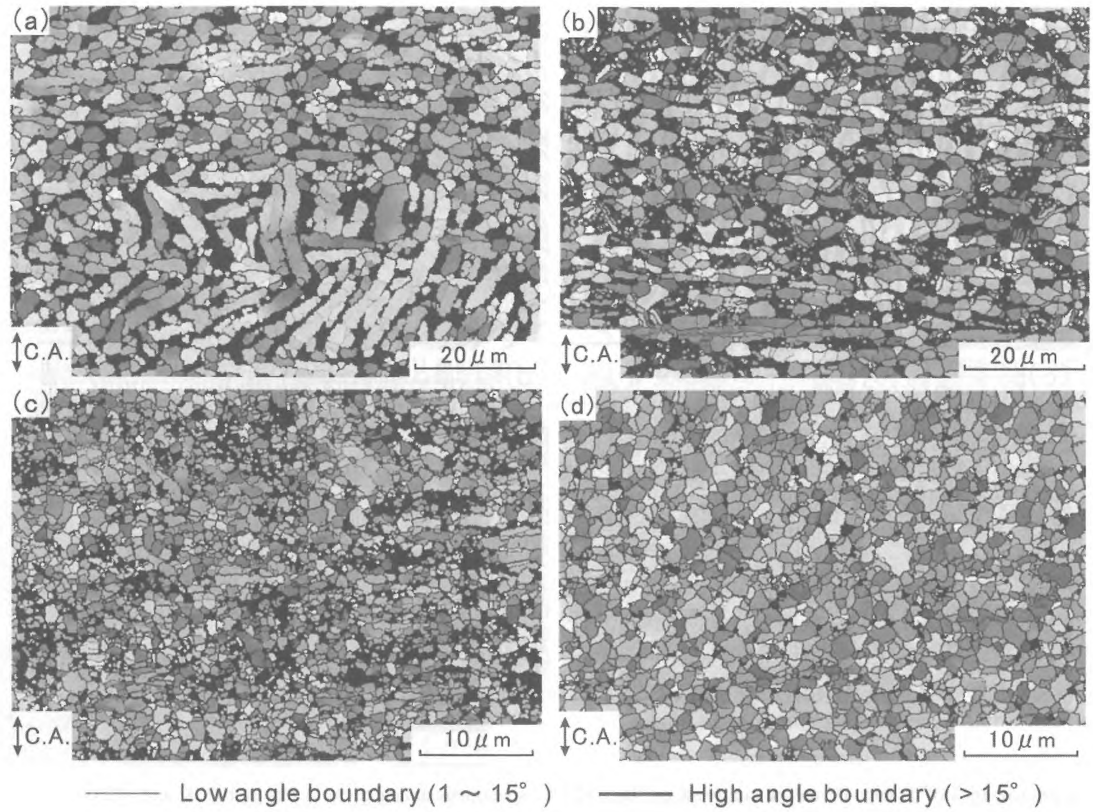

Figure 8. α orientation maps of Ti-6Al-4V water-quenched and (a) compressed at 1173K by 55% and (b) 75%, (c) compressed at 1023K by 55% and (d) 75%, respectively.

larger. This observation is consistent with the result reported by Shell and Semiatin [21]. However, it is interesting to find that α globularization is relatively faster in the deformation at 1123K than 1173K in comparison between Figs. 8(a) and (c). This is probably due to larger stored energy at 923K because of more intensive inhomogeneous deformation due to a finer initial grain size and a less degree of DRC.

Fig. 9(a) shows the changes in the misorientation across the α boundary in the W.Q. specimen compressed at 1173K. In the early stage of deformation, subgrain boundaries are formed in α plates by DRC. As further deformation is

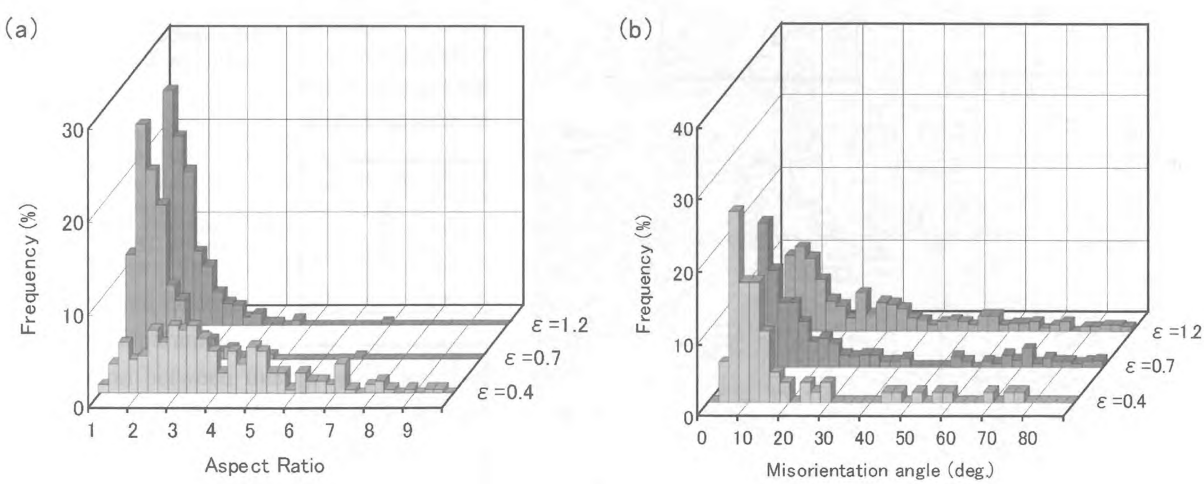

Figure 9. Changes in (a) the misorientation across the α boundary and (b) the aspect ratio of α grain in Ti-6Al-4V water-quenched and compressed at 1173K, respectively.

Table 2. α grain sizes in the initial and deformed structures.

Deformed condition	Volume fraction of α (%)	Thickness of lamellar α, w_α (μm)	Grain size of equi-axed α, d_α (μm)		
			35% compressed (ε = 0.4)	55% compressed (ε = 0.7)	75% compressed (ε = 1.2)
F.C., 1173K	40	1.75	1.66	1.81	1.64
W.Q., 1173K	43	0.94	1.39	1.25	1.13
W.Q., 1123K	76	0.89	-	0.72	0.71

applied, the misorientation of α grain boundaries increases gradually, resulting in the transition of α boundaries from low-angle to high-angle ones. This change is attributed to continuous DRX of α phase. It was also confirmed that β matrix consists of fine grains bounded by high-angle boundaries by TEM. Thus, it is considered that β matrix undergoes continuous DRX in analogue to the case of Ti-10V-2Fe-3Al deformed at 923K. Fig. 9(b) shows the change in the aspect ratio of α grain in the same deformation condition. It is clear that, as deformation strain increases, the aspect ratio of α phase decreases and approaches to unity. Table 2 shows the DRX α grain size obtained in different deformation condition. When the initial α thickness is finer, the DRX α grain size is finer. Furthermore, α phase hardly exhibits grain growth during deformation. Thus, it is reasonable to conclude that α globularization occurs by continuous DRX of α and β phases.

4. Summary

Local orientation measurement techniques were applied to study the dynamic restoration mechanism in hot deformation of titanium alloys. In the β single-phase alloy, DRC is the most dominating restoration process with some operation of DRX. When the (α+β) two-phase alloys with large volume fractions of the second phase are deformed, continuous DRX occurs and the (α+β) microduplex structures containing high-angle boundaries are formed after a certain amount of deformation. Such application of DRX and manipulation of grain boundary structures are important and useful in titanium alloys as well as other duplex alloys for lowering the flow stress, improving superplasticity and obtaining ultra-fine grained structures.

Acknowledgment

The authors thank to Professor Nobuhiro Tsuji (Dept. Adaptive Machine Systems, Osaka University, Japan) for helping in the hot compression test.

REFERENCES

1) I. Weiss, S. L. Semiatin, Mater. Sci. Engng. A243 (1998) pp. 46-65.
2) Y. Kawabe, S. Muneki, *Beta Titanium Alloys in the 1990's*, (Ed. by D. Eylon, R. R. Boyer and D. A. Koss), TMS, Warrendale, U. S. A., 1993, pp. 187-197.
3) P. M. Sargent, M. F. Ashby, Scripta Metall. 16 (1982) pp. 1415-1422.
4) I. Weiss, S. L. Semiatin: V. V. Balasubrahmanyam and Y. V. R. K. Prasad, Mater. Sci. Engng. A336 (2002) pp. 150-158.
5) T. Seshacharyulu, S. C. Medeiros, W. G Frazier, Y. V. R. K. Prasad, Mater. Sci. Engng. A284 (2000) pp. 184-194.
6) R. Ding, Z. X. Guo, A. Wilson, Mater. Sci. Engng. A327 (2002) pp. 233-245.
7) F. H. Froes, C. F. Yolton, J. P. Hirth, R. Ondercin, D. Moracz, *Beta Titanium Alloys in the 1980's*, (Ed.: R. R. Boyer and R. W. Rosenberg), TMS, Warrendale, U. S. A., 1984, pp. 161-184.
8) D. G. Robertson, H. B. Mcshane, Mater. Sci. Tech. 13 (1997) pp. 459-468.
9) D. G. Robertson, H. B. Mcshane, Mater. Sci. Tech. 13 (1997) pp. 575-583.
10) A. Belyakov, H. Miura, T. Sakai, Scrpita Mater. 43 (2000) pp. 21-26.
11) A. Belyakov, H. Miura, T. Sakai, R. Kaibyshev, K. Tsuzaki, Acta Mater. 50 (2002), pp. 1547-1557.
12) A. Ohmori, S. Torizuka, K. Nagai, K. Yamada, Y. Kogo, Tetsu-to-Hagane 88(2002) pp. 857-864.
13) Z. Q. Sun, W. Y. Yang, J. J. Qi, A. M. Hu, Mater. Sci. Engng. A334 (2002) pp. 201-206.
14) T. Furuhara, Y. Toji, H. Abe, T. Maki: Mater. Sci. Forum 426-432 (2003) pp. 655-660.
15) T. Furuhara, Y. Toji, T. Maki: *Proc. of the 10th World Conference on Titianium (Ti-2003 Science and Technology)*, (Ed. by G. Lutjering and J. Albrecht), Wiley-VCH, Weinheim, 2004, pp. 1219-1226.
16) V. V. Balasubrahmanyam, Y. V. R. K. Prasad, Mater. Sci. Tech. 17 (2001) pp. 1222-1228.
17) H. Fujii, Ph. D. Thesis, Kyoto University, 1991.
18) S.V.S. Narayana Murty, S. Torizuka, K. Nagai, Mater. Sci. Engng. A 410-411 (2005) pp. 319-323.
19) T. Furuhara, B. Poorganji, H. Abe, T. Maki, JOM 59 (2007) pp. 64-67.
20) E. B. Shell, S. L. Semiatin, Metall. Meter. Trans. 30A (1999) pp. 3219-3229.